CHARACTERISTICS OF A SERIES OF HIGH SPEED HARD CHINE PLANING HULLS - PART II: PERFORMANCE IN WAVES.

D.J. Taunton, Fluid-Structure Interaction Research Group, School of Engineering Sciences, University of Southampton
D.A. Hudson, Fluid-Structure Interaction Research Group, School of Engineering Sciences, University of Southampton
R.A. Shenoi, Fluid-Structure Interaction Research Group, School of Engineering Sciences, University of Southampton

SUMMARY

An experimental investigation into the performance of high speed hard chine planing hulls in irregular waves has been conducted. A new series of models representative of current design practice was developed and tested experimentally. Measurements of the rigid body motions and accelerations were made at three speeds in order to assess the influence of fundamental design parameters on the seakeeping performance of the hulls and human factors performance of the crew, with an aim to provide designers with useful data.

Response data, such as heave and pitch motions and accelerations, are presented as probability distributions due to the non-linear nature of high speed craft motions. Additionally statistical parameters for the experimental configurations tested are provided and the most relevant measures for crew performance discussed. Furthermore, an example of the use of these statistical parameters to evaluate the vibration dose value of the crew onboard a full scale high speed planing craft is given. It is confirmed that at high speed craft motion leads to recommended maximum values of vibration dose value being exceeded after only short durations. In practice, therefore, mitigating strategies need to be developed and/or employed to reduce crew exposure to excessive whole body vibration.

NOMENCLATURE

β	Deadrise [^{o}]
∇	Displaced volume [m^3]
Δ	Displaced veight [N]
ζ	Wave amplitude [m]
θ	Pitch [°]
λ	Ship scale factor
μ	Ship heading relative to waves [°]
ω_e	Wave encounter frequency [rad/s]
ω_0	Wave frequency [rad/s]
a_z	Vertical acceleration [m/s^2]
B	Beam [m]
C_V	Speed coefficient $C_V=V/(g.B)^{0.5}$
g	Acceleration due to gravity 9.80665m/s^2
Gyy	Pitch radius of gyration [%L]
$H_{1/3}$	Significant wave height [m]
L	Length over all [m]
LCG	Longitudinal centre of gravity [%L] from transom
$L/\nabla^{1/3}$	Length-displacement ratio
t	Time [s]
T	Draught [m]
T_z	Zero crossing period [s]
V	Speed [m/s]
Z	Heave at LCG [m]

1 INTRODUCTION

The operation of small, high speed craft for military, commercial and leisure use has increased dramatically in recent years. These craft are usually of hard chine form and designed to plane. The development of light weight propulsion systems and engines has resulted in an increase in the typical operational speed of such craft.

Extensive research into material properties and construction techniques has led to stronger hulls, with the consequence that the limiting factor in practical operations is now more likely to be the people operating the vessel. Anecdotal and survey evidence from operators of high speed craft, for example that carried out by the US Navy into their special forces [1], has shown a high probability of serious injury.

The legislative framework for ‘whole body vibration’ in the European Union [2] prescribes minimum standards for the health and safety of workers exposed to vibration. Although the research under-pinning the directive was principally carried out for the land transport industry, the standards apply to all workplaces including high speed craft. When applied to accelerations typically experienced on high speed craft it is seen that recommended maximum vibration levels are exceeded in a very short time, as shown in this work. This implies a need to assess such acceleration levels for typical operations and take mitigating action where necessary. For existing craft such action may include modification to operating procedures, crew training and fitting of alternative seat configurations or ride control systems.

For new craft the opportunity exists to consider the effects of various craft design parameters on the levels of

accelerations the crew will be exposed to. However, there is little such data in the public domain. This study presents experimentally derived data for a series of high speed hard chine planing hulls in waves, in a form that may be used by designers of such craft. The experiments are described and the analysis procedure adopted detailed. Results for a range of design parameters, including length-displacement ratio and radius of gyration, together with design features, such as transverse steps, are presented. An example of the use of these data for assessing acceleration levels for a full scale craft is also included.

2 DESCRIPTION OF MODELS

The availability of experimental data for the seakeeping performance of high speed planing hulls is limited. The most significant investigations into performance of planing craft in waves are those by Fridsma [3, 4] on a series of prismatic hull forms. This investigation covered the influence of length-to-beam ratio, deadrise angle, operating speed and wave height together with trim and load. These tests were later extended by Zarnick [5] to cover a greater range of length-beam ratios.

Other seakeeping experiments of high speed planing craft include those conducted by Rosen and Garme [6, 7] on a specific hull design. The seakeeping performance of a double-chined planing hull suitable for high speed ferry applications has been investigated by Grigoropoulos [8], but the speed range is too low for small high speed craft.

A model series was therefore designed to cover the range of L/B ratios typical of high speed interceptor craft and Union Internationale Motonautique [U.I.M.) P1 Powerboats. The parent hull, designated model C, has a L/B ratio of 4.3 and a deadrise angle of 22.5^{o}. A more detailed description of the model series is given in [9]. The main parameters of the model series are summarised in table 1. Body plans and profiles of the series are illustrated in figure 1 and 2, respectively.

Model	**A**	**B**	**C**	**D**
L[m]	**2.0**	**2.0**	**2.0**	**2.0**
B[m]	**0.32**	**0.39**	**0.46**	**0.53**
T[m]	**0.06**	**0.08**	**0.09**	**0.11**
Δ [N]	**119.25**	**175.83**	**243.40**	**321.95**
$L/\nabla^{1/3}$	**8.70**	**7.64**	**6.86**	**6.25**
L/B	**6.25**	**5.13**	**4.35**	**3.77**
[β^{o}]	**22.5**	**22.5**	**22.5**	**22.5**
Gyy	**0.16L**	**0.16L**	**0.16L**	**0.16L**
LCG [%L]	**32.9**	**32.9**	**32.9**	**32.9**

Table 1: Model details.

The range of parameters investigated in this study relative to previous research on planing hull systematic series is summarised in table 3. It may be seen that the speed range investigated is higher than previously tested, however it is limited to one deadrise angle.

The models were towed by a single free to heave post, with yaw restraint, attached at the longitudinal centre of gravity by a free to pitch fitting. All models were towed from a height 1.1 times the draught above the keel [i.e. 1.1T). No under water appendages were attached to the models. No turbulence stimulation was applied to the model, as all of the test speeds were greater than the critical Reynolds' number as recommended in [10] and illustrated in [9].

3 FACILITIES AND TESTS

3.1 FACILITIES

All of the experiments were conducted in the GKN Westland Aerospace No.3 Test Tank, at their test facilities in Cowes on the Isle of Wight. The tank has the following principal dimensions:

Length: 198m

Breadth: 4.57m

Depth: 1.68m

Maximum Carriage Speed: 15m/s

The tank has a manned carriage on which is installed a dynamometer for measuring model total resistance together with computer and instrumentation facilities for automated data acquisition. The tank is fitted with an oscillatory flap-type wave maker at one end and a passive beach at the opposite end. The wave maker is computer controlled and capable of generating both regular and irregular wave spectra.

3.2 INSTRUMENTATION AND MEASUREMENTS

Heave motions were measured with a rotary potentiometer attached by a gear to a track on the heave post. The heave post was mounted at the longitudinal centre of gravity of the model. The pitch motion was measured with a rotary potentiometer in the tow fitting. A rate gyro [Silicon Sensing CRS03, Range +/- 100 deg/s] was also mounted on the tow fitting. Accelerations were measured using piezoelectric accelerometers [XBOW

CXLHF1003, Range 100g, Bandwidth 0.3-10000 Hz] at the longitudinal centre of gravity and the bow, station 9½. The accelerometers were mounted using double sided tape. The longitudinal acceleration of the towing carriage was measured using a piezoresistive accelerometer [CFX USCA-TX, Range 10g, Bandwidth DC-100Hz] mounted on the carriage. This enabled the constant speed run section to be detected during the analysis in order to maximise run length, as described in [9].

The wave system encountered during the run was measured with a stiff, sword-type, resistance probe mounted on the carriage to the side of the model and 380mm forward of its centre of gravity. Additional measurements of the wave spectrum were made using resistance wave probes mounted in the tank.

All of the carriage signals were acquired using a high speed data logger [IOTECH DaqLab 2001] at a sample rate of 5000Hz and stored on a laptop PC. Four pole Butterworth anti-aliasing filters with a cut off frequency of 2000Hz for the accelerations and 200Hz for all other signals were used. The sample rate and anti-aliasing filter frequencies were selected based on full scale requirements [11] which were then scaled by a factor of two based on scaling the time base from full scale to model scale for a nominal scale factor of λ=5.435 and rounding for convenience.

3.3 CALM WATER RESISTANCE TESTS

The models were tested in calm water at speeds from 4 to 12m/s. Measurements of centre of gravity rise, trim angle and resistance were made. The calm water performance is described in detail in [9].

3.4 IRREGULAR WAVE SEAKEEPING TESTS

The models were tested in irregular head waves at 6, 10 and 12m/s. The wave spectra selected were based on statistics from wave buoy measurements in the region around the Isle of Wight, U.K. for a 1 year period from March 2006 to March 2007, as shown in table 4. The most probable wave height and period were selected. The tests were conducted with a sea state in which the likely severity of the model motions reflected a full scale condition whereby the coxswain would not manually reduce speed in order to reduce the motions. The quality of the irregular wave spectrum was determined by comparing the wave time history measured both by a static wave probe in the tank and by the wave probe mounted on the carriage with the ideal wave spectrum, an example is shown in figure 3. In order to get a significant number of wave encounters as suggested by the ITTC guidelines on model testing [12], a number of runs have to be grouped together. It should be noted that due to the phenomenon of 'platforming', a phenomenon where the model skips across a number of waves, the number of waves encountered by the carriage mounted wave probe can be significantly greater than the number of waves encountered by the model.

Each run commenced with the recording of zero levels for all transducers. The carriage was then accelerated down the tank to the required speed. The carriage speed was determined from the time taken to pass through a 15.24m [50ft) section of the tank with automatic timing triggers at the beginning and end. At the end of the run beaches at the side of the tank were automatically lowered to calm the water. Enough time was left between runs for the waves in the tank to settle. On average this was 10 to 15 minutes.

The full range of model test configurations is summarised in table 5. This includes changes in $L/\nabla^{1/3}$, significant wave height and modal wave period. For the parent model [C), pitch radius of gyration [model C5) was also changed and the presence of one or two transverse steps [C1 and C2, respectively) studied.

4 PRESENTATION OF RESULTS

The results from the seakeeping tests have been analysed and presented as probability distributions. The same methodology implemented by Fridsma [4], Zarnick and Turner [5] and, more recently, Schleicher [13] has been adopted.

4.1 PROBABILITY DISTRIBUTIONS

Fridsma [4] stated that as a planing boat behaves in a non-linear fashion over the greater part of its range of operation the use of response amplitude operators is not valid. Instead, statistical methods should be employed in order to show the dependence of motion and acceleration responses on the test parameters. Fridsma [4] used an exponential distribution for the vertical accelerations and a Generalized Rayleigh or Cartwright and Longuet-Higgins distribution [14] for the heave and pitch motions. The Generalized Rayleigh distribution for the maxima ξ of a signal, approximates the Normal distribution for wide-banded distributions and the Rayleigh distribution for narrow-banded distributions. Thus,

$$\boldsymbol{P(\eta) = \frac{1}{(2\pi)^{1/2}} \left[\epsilon\, e^{-\frac{1}{2}\eta^2/\epsilon^2} \right.}$$

$$+(\mathbf{1}-\boldsymbol{\epsilon}^{\mathbf{2}})^{\frac{\mathbf{1}}{\mathbf{2}}}\boldsymbol{\eta}\boldsymbol{e}^{-\frac{\mathbf{1}}{\mathbf{2}}\boldsymbol{\eta}^{\mathbf{2}}}\int_{-\infty}^{\boldsymbol{\eta}(\mathbf{1}-\boldsymbol{\epsilon}^{\mathbf{2}})^{\frac{\mathbf{1}}{\mathbf{2}}}/\boldsymbol{\epsilon}}\boldsymbol{e}^{-\frac{\mathbf{1}}{\mathbf{2}}\boldsymbol{x}^{\mathbf{2}}}\,\boldsymbol{dx}\Bigg] \quad (1)$$

where $\eta = \frac{\xi}{RMS}$ and

as ε→0 resulting in a Rayleigh Distribution,

$$P(\eta) = \eta e^{-\frac{1}{2}\eta^2} \quad (2)$$

whereas for ε→1 resulting in a Normal Distribution,

$$P(\eta) = \frac{1}{[2\pi)^{\frac{1}{2}}} e^{-\frac{1}{2}\eta^2} \quad (3)$$

In the analysis of the experimental results in this study, it was found that a Gamma distribution fitted the acceleration data better than an exponential distribution. The exponential distribution is a particular case of the Gamma distribution, [when α=1). That is,

Gamma Distribution

$$P(x|\alpha,\beta) = \begin{cases} \frac{x^{\alpha-1}e^{-x/\beta}}{\beta^{\alpha}\,\Gamma[\alpha)} & ,0 \leq < \infty \\ 0, elsewhere \end{cases} \quad (4)$$

where $\Gamma(\alpha) = \int_0^{\infty} x^{\alpha-1}e^{-x}$

Exponential Distribution

$$P(x|\beta) = \begin{cases} \frac{1}{\beta}e^{-x/\beta} & ,0 \leq x < \infty \\ 0, elsewhere \end{cases} \quad (5)$$

The analysis process adopted is as follows:

1) The test runs which comprise a single test condition are loaded and the mean of each run is removed before the runs joined to produce a single time trace for a given test condition.
2) A peak detection algorithm, as used by Allen et al. [11], is used to find the peaks in the time trace. These peaks are grouped into either maxima or minima. For the case of accelerations the minima are used because they represent the deceleration on impact with the water.
3) The maxima or minima are sorted into ascending order.
4) The proportion, r, of negative maxima to total maxima is determined, or in the case of minima the proportion of positive minima to total minima determined.
5) The r value is used to determine the spectral width of the spectrum, ε.

$$\varepsilon^2 = 1 - [1-2r)^2 \quad (6)$$

6) The sorted maxima or minima are grouped into 15 equal width bins and a histogram plotted.
7) For the wave height distributions and vessel motion a Cartwright and Longuet-Higgins probability density function [14] is used to determine the expected values for the particular condition. For the vertical acceleration distributions a Gamma probability density function is used to determine the expected values.
8) A χ^2 goodness of fit calculation is determined.

4.2 STATISTICS

The use of statistics as a means to compare different hullforms in the same sea state is useful, as it provides a single number with which to compare the hulls. A number of the statistics commonly used are required for assessing the performance of high speed planing craft under the EU directive on whole body vibration [2]. However, it should be noted that under the EU directive acceleration values need to be weighted and this is only possible for data acquired at full scale. Statistical measures relevant to high speed craft motions may thus be summarised as,

Root mean square

$$rms = \left[\frac{1}{N}\sum x^2(i)\right]^{1/2} \quad (7)$$

Root mean quad

$$rmq = \left[\frac{1}{N}\sum x^4(i)\right]^{1/4} \quad (8)$$

Vibration dose value

$$VDV = \left[\frac{Ts}{N}\sum x^4(i)\right]^{1/4} \quad (9)$$

Crest Factor

Is the peak value divided by the rms.

4.3 VIBRATION DOSE VALUE AND HUMAN FACTORS.

Traditionally naval architects have used statistics such as motion sickness incidence [MSI), subjective magnitude [SM) and motion induced interruptions [MII) as measures of human performance [15]. These measures are either not applicable to small high speed craft, where the crew are usually seated, or have been superseded by more recent and relevant measures.

For example, the measure of motion sickness now uses the motion sickness dose value described in ISO 2631-1 [16]. Motion induced interruptions are not usually applicable to seated crew and the subjective magnitude measure could now be replaced by the vibration dose value [VDV) as described in ISO 2631-1 or the spinal response acceleration dose described in ISO-2631-5 [17]. Whilst these new measures were not developed specifically for assessing the human performance on board ships, they have been developed to quantify human performance in a variety of transport methods and this facilitates ready comparison between them and between human performance in different occupations. There has been debate recently as to the applicability of these measures to the assessment of small boat performance [18, 19], especially since VDV has been implemented as one of the measures in an EU directive on whole body vibration [2]. The reasoning behind the debate on the applicability of VDV is that there is a high prevalence of injury among high speed craft crew [1] and vibration dose value was developed for quantifying performance degradation rather than injury. The magnitude of the accelerations used to validate the vibration dose value model for use in human factors were also much smaller than those typically encountered in high speed craft operation.

A means of comparing the performance of different hullforms is still required, however, and until a more suitable method of evaluating high speed craft is developed and validated, VDV is probably the most suitable measure of performance. A number of investigations have been conducted into the vibration dose values of different vehicles, including powerboats and RIBs [20, 21]. A pilot study into the human performance degradation due to simulated slamming conducted by Wolk [22] concluded that human performance reduced with increasing slam magnitude and frequency.

5 DISCUSSION OF RESULTS

Example motion and acceleration time traces are presented in figures 4 to 7 for model C in configuration 12 of table 5. That is, at a model speed of 6.25m/s in a JONSWAP spectrum corresponding to a full scale $H_{1/3}$ of 0.5m and modal period of 6s, based on a nominal scale factor of λ=5.435. The full scale speed for this condition is thus 14.57 m/s, or 28.32 knots. It can be seen from figure 4 that the heave motion is similar in frequency to the wave amplitude, which is supported by the power spectral density plot in figure 8. In comparison, the vertical acceleration time traces shown in figures 6 and 7 illustrate that the trace consists of repeated shock impacts. The example acceleration power spectral density in figure 9 shows a second peak at an encounter frequency of 1.5Hz.

Figures 10 to 16 show examples of the histograms and fitted probability distribution functions for wave height, heave maxima, heave minima, pitch maxima, pitch minima and centre of gravity and bow acceleration minima for the parent model [C) at one speed and travelling in one irregular sea state. For all the model configurations tested [table 5), all parameters for the relevant probability distributions are presented in table 6. These data allow the probability distribution for any model configuration in table 5 to be re-created in a manner similar to the examples presented in figure 10 to 16. Once the probability distribution for the motion responses is known, the probability of any motion variable exceeding a particular value may readily be found. These data are thus of direct use for designers of such high speed craft.

A linear regression model has been fitted to the experimental data to show the relationship between length-displacement ratio, speed coefficient C_v and RMS vertical accelerations at the longitudinal centre of gravity [LCG) and the bow. The results are plotted in figure 17 and 18 and the regression equations are given as,

$$\boldsymbol{a_z\, rms = C + C1 \times \left(\frac{L}{\nabla^{\frac{1}{3}}}\right)^2 + C2 \times {C_V}^2 + C3 \times \left(\frac{L}{\nabla^{\frac{1}{3}}}\right)^2 {C_V}^2 + C4 \times \left(\frac{L}{\nabla^{\frac{1}{3}}}\right)^2 C_V + C5 \times \left(\frac{L}{\nabla^{\frac{1}{3}}}\right) {C_V}^2 + C6 \times \left(\frac{L}{\nabla^{\frac{1}{3}}}\right) + C7 \times C_V + C8 \times \left(\frac{L}{\nabla^{\frac{1}{3}}}\right) C_V} \quad (10)$$

	RMS Acceleration at LCG	RMS Acceleration at Bow
C	154.5	291.6
C1	2.6	4.9
C2	9.8	17.8
C3	0.2	0.3
C4	-1.5	-2.8
C5	-2.6	-4.9
C6	-41.2	-77.2
C7	-85.3	-155.6
C8	23.0	43.0

Table 2: Regression coefficients for RMS vertical acceleration in equation 10.

The influence of transverse steps on the RMS vertical accelerations for model C at three speeds is presented in figure 19. This figure indicates that steps have virtually no influence on the RMS accelerations.

The influence of wave height on the RMS accelerations for model C are presented in figure 20. This shows a non linear relationship for the LCG accelerations, with little change in acceleration for increasing wave height and an almost linear relationship for the bow accelerations.

6 DESIGN APPLICATIONS

In order to allow the model data to be used to predict the human performance onboard a full scale vessel, tables of RMS and RMQ accelerations are presented in table 7. The RMS and RMQ values have been weighted using the weighting W_b as described in ISO 2631-1 [16]. This process involved scaling the model test data to a nominal full scale, applying the weighting and then scaling the weighted data back to model scale. The weighted RMS and RMQ accelerations were next calculated at the longitudinal centre of gravity and bow. Using the RMQ it is possible to calculate the VDV as,

$$VDV = RMQ \cdot t^{1/4} \qquad (11)$$

The duration, t, is a function of scale factor, $R^{0.5}$, which means that it is possible to calculate the VDV for any other scale of vessel by multiplying the RMQ by $[t \cdot R^{0.5})^{1/4}$.

The estimated time to exceed a given VDV limit, such as the daily exposure action value [9.1 $m/s^{1.75}$) and the daily exposure limit [21 $m/s^{1.75}$) given in the EU Directive on whole body vibration [2] can be calculated using equation 12,

$$Time\ to\ limit = \frac{VDV\ Limit^4 * Duration}{Measured\ VDV^4} \qquad (12)$$

An example to illustrate how the model data may be used to determine full-scale seakeeping performance and assessment against the EU directive on whole body vibration [2] is given below:

The example given is for a full scale vessel similar to model C2 with a length of 15m. This results in a scale factor of λ=7.5. The vessel has a design speed of 65 knots.

1) Select the most appropriate model configuration from table 5, in this case configuration 32.
2) Use the corresponding values of weighted RMS and RMQ vertical accelerations from table 7. In this example RMS at LCG is 8.09 ms^{-2} and the RMQ at LCG is 10.84 ms^{-2}. The duration of the model runs was 11.68 s.
3) The model run duration is scaled from model to full scale. $T_{full}=T_{model}\times\lambda^{0.5}$, in this case,
   $T_{full}=11.68 \times 2.74$
   $T_{full}=31.99$ s
4) The full scale vibration dose value [VDV) can then be calculated using equation 11 as

   $$VDV_{full} = 10.84 \times 31.99^{1/4}$$

   $$VDV_{full}=25.78\ ms^{-1.75}$$

5) The time to exceed the 8 hour daily exposure limit, given in the EU directive [2], of 21 $ms^{-1.75}$ is then calculated from equation 12:

   $$time\ to\ limit = \frac{21^4 \times 31.99}{25.78^4}$$

   Time to the VDV limit of 21 m $s^{-1.75}$ = 14.09s

7 CONCLUSIONS

An extensive experimental investigation into the motions of small high speed craft in waves has been completed through model scale testing. A new series of hard chine planing hulls representative of modern practice was designed to allow the influence of $L/\nabla^{1/3}$ on the behaviour of such craft in waves to be studied. The models were tested at three speeds. In addition a limited investigation into the effects of transverse steps, radius of gyration, wave height and wave period on the craft motions in waves was undertaken.

Due to the non-linearity of planing craft motions in waves probability distributions are fitted to heave and

pitch motions and accelerations at the centre of gravity and bow. These distributions allow comparisons between model configurations and prediction of occurrence of extremes to be made. Such data are presented in a form useful to designers selecting appropriate hull forms.

Statistical data for each configuration tested also enables predictions of measures of human performance for crew onboard such small high speed craft. An example of the use of these data for predicting vibration dose value for crew at full scale is given. This confirms that exposure to these levels of vibration onboard small, fast craft leads to crew exceeding rapidly the limits prescribed in EU legislation.

For designers of high speed craft this implies that mitigation of the levels of vibration should be sought. Such mitigation may comprise, but is not limited to, hull design, active ride control systems, seat design, training methods and operating procedures.

8 REFERENCES

[1] W. ENSIGN, J. A. HODGDON, W. K. PRUSACZYK, D. SHAPIRO, and M. LIPTON, 'A Survey of Self-Reported injuries Among Special Boat Operators', Naval Health Research Center, Report No. 00-48, 2000.

[2] 'DIRECTIVE 2002/44/EC OF THE EUROPEAN PARLIAMENT AND OF THE COUNCIL of 25 June 2002 on the minimum health and safety requirements regarding the exposure of workers to the risks arising from physical agents [vibration) [sixteenth individual Directive within the meaning of Article 16[1) of Directive 89/391/EEC)'. Council of European Union, Ed., 2002.

[3] G. FRIDSMA, 'A systematic study of the rough-water performance of planing boats', Stevens Institute of Technology, Report No. 1275, 1969.

[4] G. FRIDSMA, 'A systematic study of the rough-water performance of planing boats [Irregular Waves - Part II)', Stevens Institute of Technology, Report No. 1495, 1971.

[5] E. E. ZARNICK and C. R. TURNER, 'Rough water performance of high length to beam ratio planing boats', David W. Taylor Naval Ship Research and Development Center, Bethesda, Maryland, Report No. DTNSRDC/SPD-0973-01, 1981.

[6] A. ROSEN, 'Loads and responses for planing craft in waves', in *Division of naval Systems, Aeronautical and Vehicle Engineering*. PhD Stockholm: KTH, 2004.

[7] A. ROSEN and K. GARME, 'Model experiment addressing the impact pressure distribution on planing craft in waves', *Transactions of the Royal Institution of Naval Architects, Volume 146*, 2004.

[8] G. J. GRIGOROPOULOS, S. HARRIES, D. P. DAMALA, L. BIRK, and J. HEIMANN, 'Seakeeping assessment for high-speed monohulls - A comparative study.', *Int. Marine Design Conf. IMDC, Volume 1, pp. 137-148*, 2003.

[9] D. J. TAUNTON, D. A. HUDSON, and R. A. SHENOI, 'Characteristics of a series of high speed hard chine planing hulls - Part I: Performance in calm water.', *International Journal of Small Craft Technology, Volume 152, Part B2, pp55-75*, 2010.

[10] 'Testing and Extrapolation Methods, High Speed Marine Vehicles, Resistance Test', in *ITTC - Recommended Procedures and Guidelines*, 2002, p. 18.

[11] D. P. ALLEN, D. J. TAUNTON, and R. ALLEN, 'A study of shock impacts and vibration dose values onboard highspeed marine craft', *International Journal of Maritime Engineering, Volume 150, pp. 10*, 2008.

[12] 'Testing and Extrapolation Methods, High Speed Marine Vehicles, Sea Keeping Tests', in *ITTC - Recommended Procedures and Guidelines*. vol. 7.5-02-05-04, 2002, p. 13.

[13] D. M. SCHLEICHER, 'Regarding statistical relationships for vertical accelerations of planing monohulls in head seas', in *High speed craft - ACV's, WIG's & Hydrofoils*. London: RINA, 2006.

[14] D. E. CARTWRIGHT and M. S. LONGUET-HIGGINS, 'The statistical distribution of the maxima of a random function', *Proceedings of the Royal Society of London. Series A, Mathematical and Physical Sciences, Volume 237, pp. 21*, 1956.

[15] A. LLOYD, 'Seakeeping: Ship Behaviour in Rough Weather', Revised ed.: ARJM Lloyd, ISBN 0953263401, 1998.

[16] INTERNATIONAL ORGANISATION FOR STANDARDISATION, 'Mechanical vibration and shock - Evaluation of human exposure to

whole-body vibration -Part 1: General requirements.', ISO 2631-1:1997[E).

[17] INTERNATIONAL ORGANISATION FOR STANDARDISATION, 'Mechanical vibration and shock —Evaluation of human exposure to wholebody vibration — Part 5: Method for evaluation of vibration containing multiple shocks.', ISO 2631-5:2003[E).

[18] R. CRIPPS, S. REES, H. PHILLIPS, C. CAIN, D. RICHARDS, and J. CROSS, 'Development of a crew seat system for high speed craft', in *Seventh International Conference on Fast Sea Transportation, FAST 2003*. Ischia, Italy, 2003.

[19] R. GOLLWITZER and R. PETERSON, 'Repeated Water Entry Shocks on High-Speed Planing Boats', Dahlgren Division, Naval Surface Warfare Center, Panama City, Report No. CSS/TR-96/27, 1995.

[20] C. H. LEWIS and M. J. GRIFFIN, 'A comparison of evaluations and assessments obtained using alternative standards for predicting the hazards of whole-body vibration and repeated shocks.', *Journal of Sound and Vibration, Volume 215, pp. 915-926*, 1998.

[21] G. S. PADDAN and M. J. GRIFFIN, 'Evaluation of whole-body vibration in vehicles', *Journal of Sound and Vibration, Volume 253, pp. 195-213*, 2002.

[22] H. WOLK and J. F. TAUBER, 'Man's Performance Degradation during Simulated Small Boat Slamming ', Naval Ship Research and Development Center, Bethesda, Report No. 4234, 1974.

Series	**L/B**	**β**	**C_V**
Series 65[7]	**3.2-9.26** 2.32-9.28	**14.8-27.9** 16.3-30.4	**0 - 3.03** 0 - 1.432
Series 62[6]	2.0 -7.0	12.5	**0.087-4.116**
Metcalf et al.[8]	3.24 – 4.47	16.61, 20	0.28 – 2.634
Fridsma[8,10]	4-6	10-30	0 - 4.0
Zarnick[11]	7,9	10-30	1.57 – 3.15
Southampton [present work)	3.7 – 6.2	22.5	1.75 – 6.77

Table 3: Planing craft systematic series.

Significant Wave height [m]											
	5	-	-	-	-	-	-	-	-	-	-
	4.5	-	-	-	-	-	-	-	-	-	-
	4	-	-	-	-	-	-	1	-	-	-
	3.5	-	-	-	-	-	9	12	-	-	-
	3	-	-	-	-	6	81	16	-	-	-
	2.5	-	-	-	-	140	239	73	8	3	-
	2	-	-	-	27	848	303	82	13	3	1
	1.5	-	-	-	869	1020	257	66	21	15	10
	1	-	-	804	2870	686	242	112	52	34	20
	0.5	-	-	3913	3514	736	257	109	37	9	2
		1	**2**	**3**	**4**	**5**	**6**	**7**	**8**	**9**	**10**

Zero Crossing Period [s]

Number of recordings=17520

Table 4: Wave statistics compiled from directional waverider buoys in and around the Solent, U.K. for 12 months from March 2006. [Locations included: Boscombe, Hayling Island, Milford-on-Sea, Sandown Bay, Weymouth and Rustington].

Configuration	Model	C_V	$H_{1/3}$	T	Gyy
1	A	3.53	0.092	1.72	0.16
2	A	5.7	0.092	1.72	0.16
3	A	6.8	0.092	1.72	0.16
4	A	6.8	0.092	2.57	0.16
5	B	3.2	0.092	1.72	0.16
6	B	5.16	0.092	1.72	0.16
7	B	6.24	0.092	1.72	0.16
8	B	6.16	0.046	1.72	0.16
9	B	6.16	0.092	1.72	0.16
10	B	6.16	0.092	2.57	0.16
11	B	3.19	0.184	2.57	0.16
12	C	2.94	0.092	2.57	0.16
13	C	4.71	0.092	2.57	0.16
14	C	5.67	0.092	2.57	0.16
15	C	5.67	0.092	1.72	0.16
16	C	5.67	0.046	2.57	0.16
17	C	5.67	0.138	2.57	0.16
18	C	5.67	0.046	2.57	0.16
19	C	2.94	0.092	1.72	0.16
20	D	2.74	0.092	1.72	0.16
21	D	4.44	0.092	1.72	0.16
22	D	5.29	0.092	1.72	0.16
23	D	5.29	0.092	2.57	0.16
24	D	2.74	0.184	1.72	0.16
25	D	2.74	0.184	2.57	0.16
26	D	2.74	0.092	2.57	0.16
27	C1	2.94	0.092	2.57	0.16
28	C1	4.71	0.092	2.57	0.16
29	C1	5.67	0.092	2.57	0.16
30	C2	2.94	0.092	2.57	0.16
31	C2	4.71	0.092	2.57	0.16
32	C2	5.67	0.092	2.57	0.16
33	C2	5.67	0.092	1.72	0.16
34	C4	2.94	0.092	2.57	0.16
35	C4	4.71	0.092	2.57	0.16
36	C4	5.67	0.092	2.57	0.16
37	C4	5.67	0.092	1.72	0.16
38	C5	2.94	0.092	2.57	0.2
39	C5	4.71	0.092	2.57	0.2
40	C5	5.67	0.092	2.57	0.2
41	C5	5.67	0.092	1.72	0.2

Table 5: Seakeeping model test configurations

	Heave Maxima			Heave Minima			Pitch Maxima			Pitch Minima			Az		Bz	
#	Mean	RMS	r	Mean	RMS	r	Mean	RMS	r	Mean	RMS	r	α	β	α	β
1	0.024	0.032	0.079	-0.022	0.025	0.000	0.531	0.709	0.145	-0.548	0.744	0.145	1.974	4.615	1.554	18.430
2	0.020	0.027	0.172	-0.020	0.021	0.000	0.390	0.502	0.148	-0.414	0.461	0.018	2.786	7.564	2.899	19.889
3	0.018	0.025	0.146	-0.019	0.021	0.000	0.331	0.497	0.154	-0.385	0.513	0.128	2.675	9.921	2.964	21.319
4	0.028	0.036	0.025	-0.028	0.031	0.025	0.457	0.575	0.122	-0.545	0.598	0.000	2.236	7.624	1.359	31.010
5	0.027	0.035	0.000	-0.026	0.029	0.015	0.507	0.605	0.029	-0.566	0.635	0.029	1.716	5.852	1.044	27.601
6	0.029	0.041	0.161	-0.030	0.032	0.000	0.381	0.488	0.132	-0.428	0.485	0.000	3.267	6.825	2.305	23.205
7	0.037	0.050	0.114	-0.037	0.041	0.000	0.346	0.547	0.176	-0.428	0.595	0.147	3.544	6.818	3.321	15.432
8	0.023	0.030	0.042	-0.021	0.023	0.000	0.301	0.374	0.042	-0.277	0.390	0.167	2.890	3.825	2.100	13.552
9	0.037	0.050	0.114	-0.037	0.041	0.000	0.346	0.547	0.176	-0.428	0.595	0.147	3.544	6.818	3.321	15.432
10	0.060	0.076	0.069	-0.061	0.068	0.017	0.520	0.671	0.114	-0.652	1.052	0.157	1.684	10.819	1.327	29.169
11	0.072	0.096	0.111	-0.075	0.082	0.037	0.980	2.009	0.182	-1.266	2.253	0.273	1.269	9.959	1.153	29.974
12	0.038	0.052	0.120	-0.036	0.043	0.079	1.273	2.654	0.215	-2.056	3.039	0.165	1.657	3.094	1.095	13.355
13	0.039	0.056	0.139	-0.040	0.045	0.028	1.259	1.530	0.051	-1.335	1.755	0.053	1.538	6.636	1.461	19.565
14	0.051	0.068	0.130	-0.055	0.058	0.000	2.229	2.833	0.042	-2.929	3.767	0.125	1.864	11.560	1.148	38.674
15	0.029	0.043	0.200	-0.032	0.036	0.033	0.894	1.217	0.120	-1.363	3.067	0.160	1.644	11.874	1.888	27.162
16	0.024	0.033	0.097	-0.025	0.031	0.033	0.795	1.007	0.069	-0.941	1.087	0.034	2.810	2.879	1.780	12.864
17	0.069	0.094	0.190	-0.080	0.087	0.000	1.602	1.874	0.043	-1.239	2.203	0.261	2.043	13.063	0.700	77.727
18	0.024	0.033	0.097	-0.025	0.031	0.033	0.795	1.007	0.069	-0.941	1.087	0.034	2.810	2.879	1.780	12.864
19	0.031	0.040	0.101	-0.030	0.032	0.000	1.252	1.473	0.065	-1.414	1.570	0.011	1.577	5.475	1.060	24.211
20	0.028	0.036	0.108	-0.027	0.029	0.000	0.496	0.594	0.078	-0.546	0.629	0.046	1.728	4.090	1.267	16.655
21	0.034	0.049	0.167	-0.034	0.037	0.000	0.411	0.553	0.106	-0.483	0.626	0.128	2.601	5.016	2.000	17.735
22	0.053	0.063	0.114	-0.050	0.061	0.114	0.971	1.327	0.093	-1.492	2.039	0.070	3.565	5.567	1.458	26.223
23	0.036	0.044	0.042	-0.038	0.041	0.000	0.600	0.791	0.106	-0.749	0.940	0.064	1.472	12.335	1.695	19.778
24	0.047	0.068	0.063	-0.048	0.053	0.061	0.705	0.957	0.069	-0.941	1.107	0.033	1.253	11.924	1.052	35.540
25	0.080	0.101	0.130	-0.073	0.081	0.000	0.901	1.118	0.208	-1.227	1.433	0.000	1.416	7.227	1.171	23.770
26	0.039	0.046	0.070	-0.041	0.050	0.057	1.508	1.912	0.135	-1.912	2.245	0.014	1.347	3.344	1.225	10.293
27	0.030	0.036	0.026	-0.027	0.036	0.165	1.223	1.465	0.076	-1.419	1.704	0.051	2.318	1.620	1.458	7.555
28	0.045	0.057	0.114	-0.047	0.051	0.000	1.329	1.633	0.125	-1.611	1.790	0.026	1.666	7.415	1.138	28.501
29	0.048	0.058	0.043	-0.052	0.058	0.000	1.142	1.393	0.111	-1.287	1.507	0.037	2.005	9.101	1.433	30.501
30	0.032	0.040	0.053	-0.030	0.037	0.065	1.240	1.498	0.048	-1.387	1.732	0.072	1.706	2.344	1.354	9.034
31	0.036	0.045	0.028	-0.040	0.045	0.000	1.402	1.587	0.000	-1.563	1.780	0.027	1.707	6.208	1.209	25.175
32	0.040	0.052	0.036	-0.044	0.050	0.037	1.419	1.658	0.107	-1.915	3.133	0.071	3.114	5.326	1.501	26.636
33	0.035	0.045	0.094	-0.038	0.041	0.000	1.426	1.809	0.063	-1.864	3.808	0.125	3.590	6.937	2.020	30.469
34	0.037	0.048	0.107	-0.035	0.042	0.027	1.562	1.878	0.053	-1.867	2.231	0.039	1.326	3.577	1.073	13.219
35	0.039	0.052	0.075	-0.042	0.047	0.025	1.322	1.709	0.150	-1.628	1.834	0.025	2.750	4.448	1.913	19.202
36	0.048	0.061	0.083	-0.051	0.057	0.000	1.070	1.341	0.077	-1.318	1.906	0.111	1.640	10.612	1.005	38.385
37	0.046	0.057	0.036	-0.048	0.052	0.000	1.300	1.568	0.034	-1.310	1.933	0.107	3.906	5.306	1.221	39.094
38	0.036	0.045	0.107	-0.034	0.040	0.014	1.166	2.212	0.236	-1.860	2.750	0.159	1.766	2.579	1.441	8.926
39	0.051	0.059	0.029	-0.050	0.056	0.029	1.706	1.943	0.029	-2.200	2.694	0.000	2.254	4.887	1.266	22.189
40	0.061	0.073	0.000	-0.061	0.066	0.000	1.382	1.563	0.000	-1.431	2.188	0.120	1.991	10.047	1.732	23.107
41	0.033	0.046	0.103	-0.033	0.040	0.036	0.970	1.399	0.077	-1.287	1.811	0.080	2.773	6.590	2.775	15.133

Table 6: Distribution parameters

#	Duration [s]	Weighting	LCG			Bow		
			Crest factor	RMSw	RMQw	Crest factor	RMSw	RMQw
1	34.39	B	7.61	4.79	7.83	5.95	10.67	17.13
2	21.94	B	4.64	8.48	12.51	4.74	15.75	24.58
3	14.6	B	4.75	9.42	13.51	4.28	16.33	24.73
4	19.42	B	5.32	7.73	11.19	5.08	14.84	23.41
5	31.73	B	5.56	4.94	7.69	5.69	11.15	18.29
6	20.73	B	4.72	8.82	12.85	4.48	16.42	24.72
7	13.36	B	4.27	9.3	13.05	4.58	15.86	22.63
8	8.98	B	3.9	5.72	7.98	4.66	11.1	16.75
9	13.36	B	4.27	9.3	13.05	4.58	15.86	22.63
10	28.19	B	5.33	8.29	12.25	5.33	14.62	23.16
11	16.84	B	5.79	5.57	9.09	6.12	11.65	20.05
12	47.63	B	7.23	2.96	5	7.63	7.31	12.89
13	17.73	B	4.55	5.76	8.62	5.12	12.05	19.22
14	11.06	B	4.18	8.51	12.65	5.24	15.38	24.58
15	10.25	B	4.11	8.48	12.39	4.49	15.08	22.75
16	11.8	B	3.47	5.06	6.85	3.94	10.67	15.73
17	10.9	B	4.97	9.07	13.91	6.62	18.32	31.57
18	11.8	B	3.47	5.06	6.85	3.94	10.67	15.73
19	47.54	B	7.38	4.32	6.96	5.63	10.44	16.58
20	34.67	B	7.85	3.88	6.64	6.33	9.91	16.89
21	22.32	B	4.79	6.48	9.27	4.42	13.22	19.91
22	25.95	B	4.06	8.11	11.06	5.4	14.87	22.74
23	23.44	B	4.27	7.96	11.27	4.39	14.26	20.64
24	17.44	B	5.55	6.42	10.5	6.83	14.39	24.2
25	16.98	B	6.75	4.84	8.79	6.07	10.95	19.67
26	46.87	B	4.9	2.67	4.02	5.07	6.6	10.42
27	47.26	B	4.31	2.36	3.26	4.87	6.33	9.4
28	18.11	B	5.33	6.17	9.34	4.53	13.15	20.18
29	11.29	B	4.26	7.92	11.71	4.24	15.48	23.16
30	47.65	B	4.24	2.6	3.59	5.27	6.58	10.01
31	17.26	B	3.91	6.22	8.7	4.61	13.19	19.83
32	11.68	B	3.32	8.09	10.84	3.74	16	22.81
33	11.62	B	3.74	9.59	13.18	4.16	18.78	27.28
34	46.71	B	6.19	2.93	4.64	6.84	7.65	13.08
35	18.34	B	4.29	6.37	9.23	4.32	13.91	20.71
36	10.97	B	4.49	7.93	11.82	3.96	15.24	22.81
37	12.33	B	4.02	8.43	11.78	5.01	16.75	25.16
38	47.54	B	5.11	2.58	3.74	6.42	6.27	9.85
39	18.3	B	4.25	5.89	8.59	5.12	12.04	19.1
40	11.27	B	4.22	7.66	10.62	4.33	14.45	22.14
41	11.2	B	4	7.46	10.4	5.37	12.82	19.75

Table 7: Weighted vertical acceleration RMS and RMQ

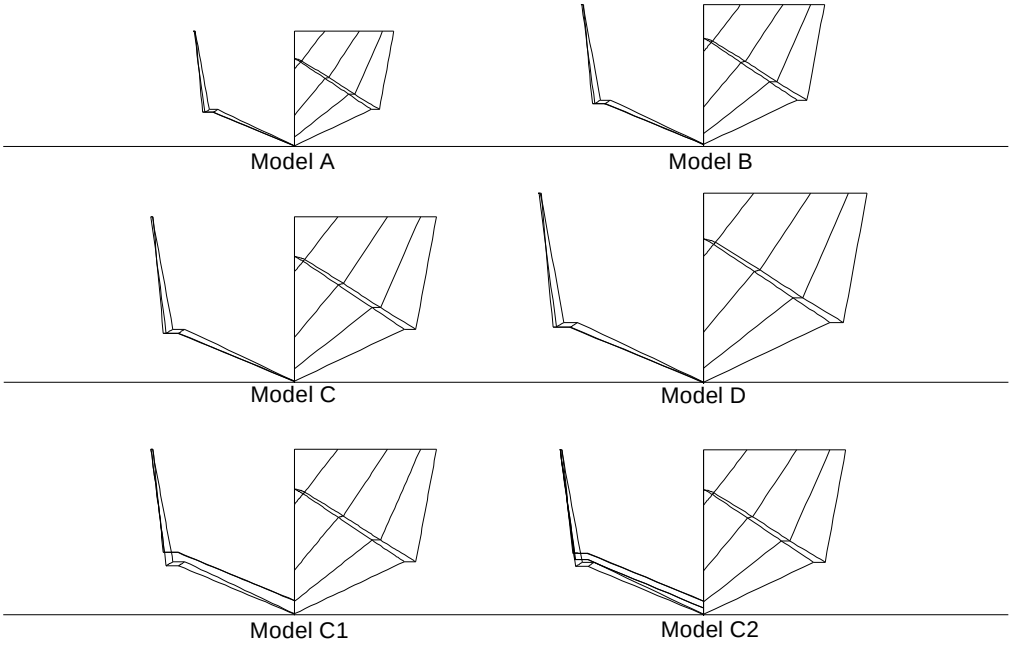

Figure 1: Model body plans [Models A, B; C, D; C1, C2)

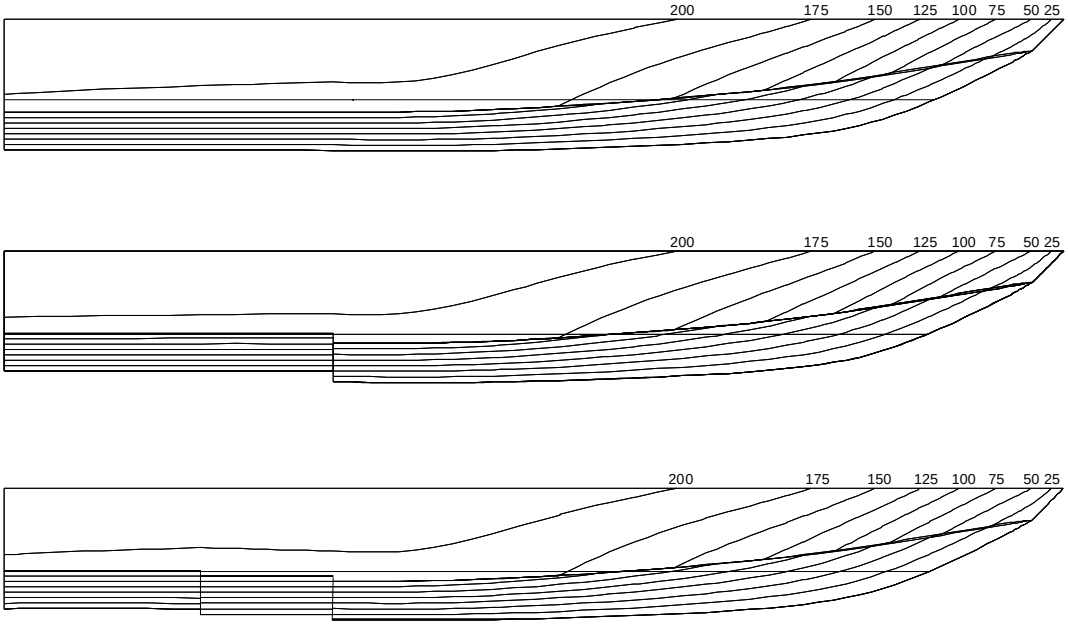

Figure 2: Model profiles [Models A-D, Model C1, Model C2)

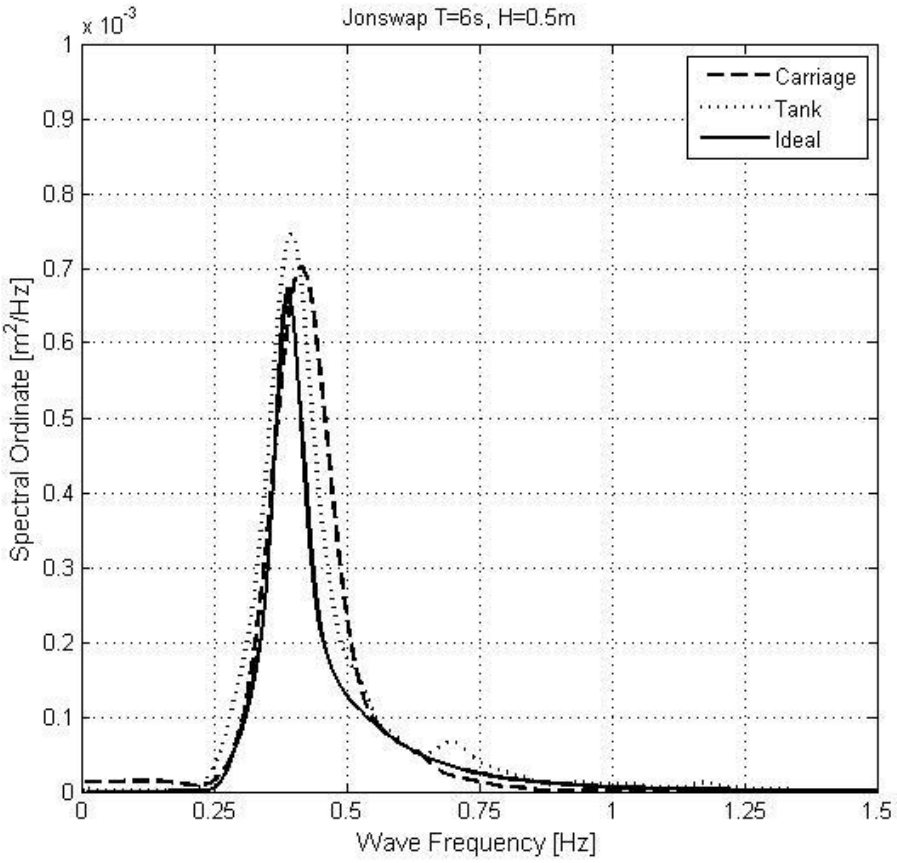

Figure 3: Example wave spectra obtained from a probe mounted on the carriage, a static probe in the tank and the ideal spectrum. Full scale JONSWAP T_z=6s, $H_{1/3}$=0.5m, [Tz=2.57s, $H_{1/3}$=0.09m model scale).

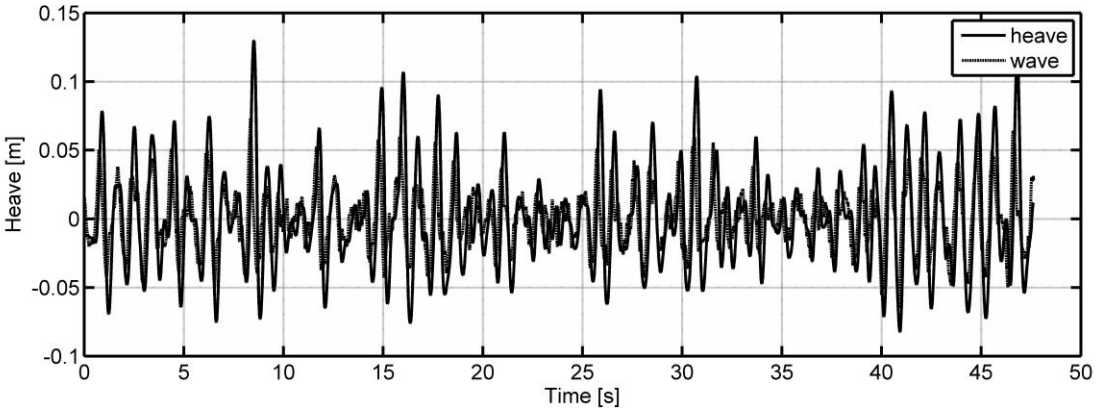

Figure 4: Example heave motion time trace, run configuration 12

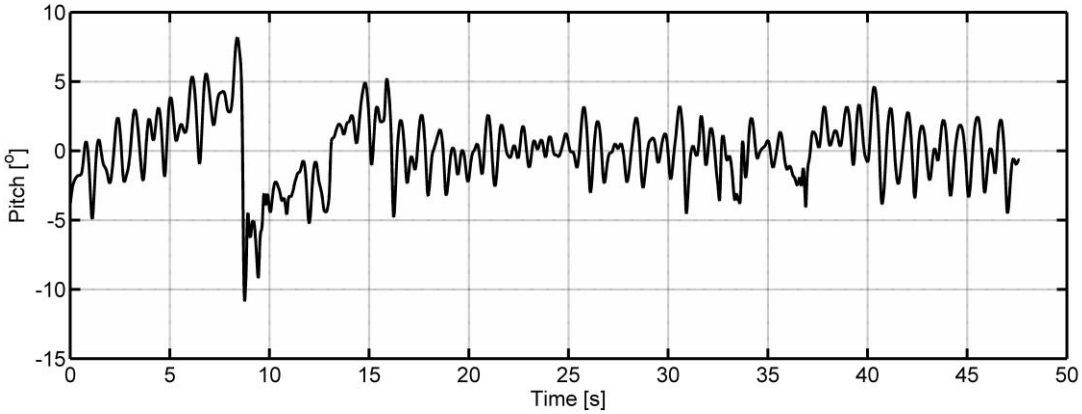

Figure 5: Example pitch motion time trace, run configuration 12

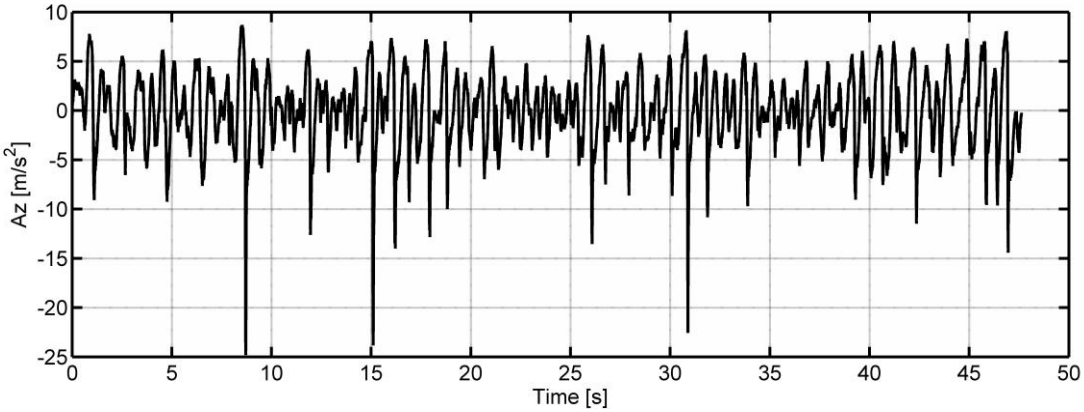

Figure 6 : Example CG acceleration time trace, run configuration 12

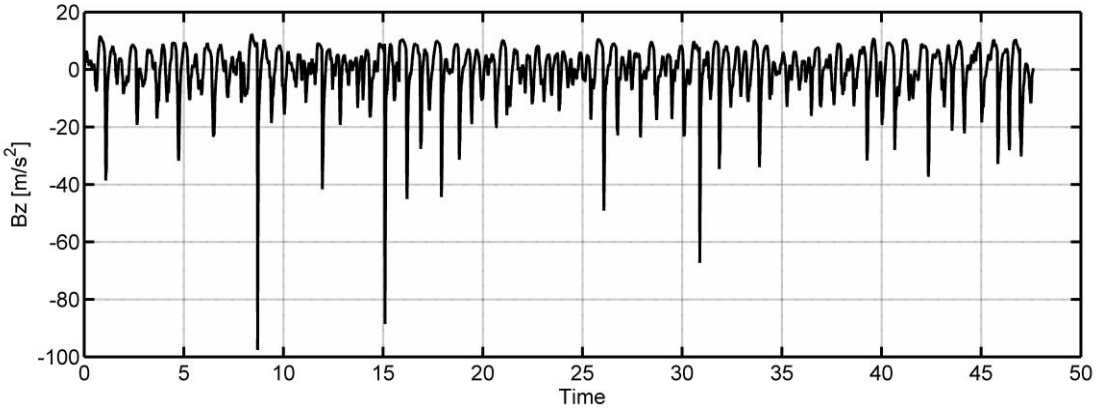

Figure 7: Example bow acceleration time trace, run configuration 12

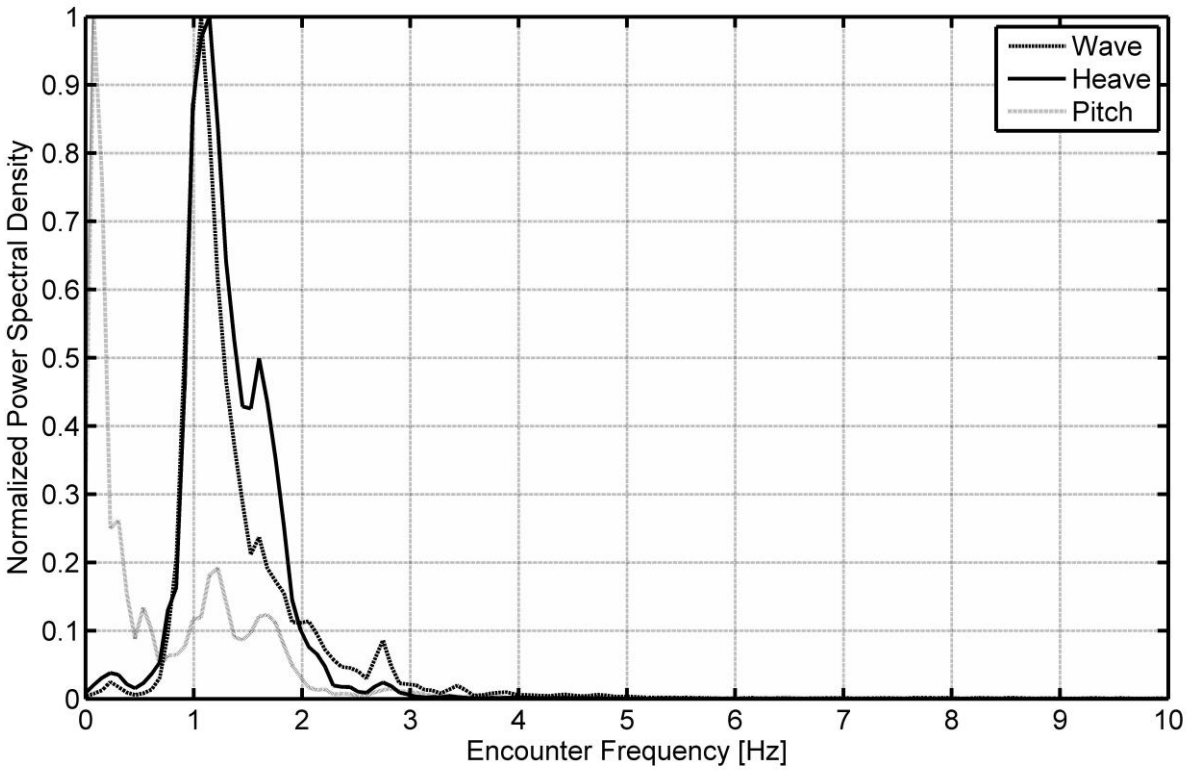

Figure 8: Example motion power spectral density, run configuration 12

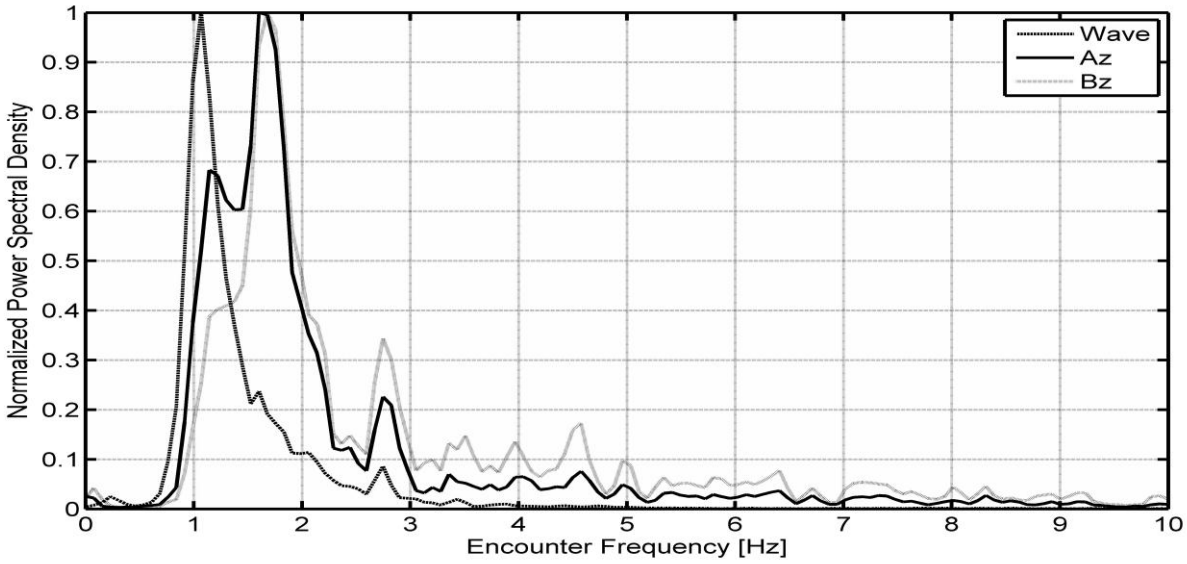

Figure 9: Example vertical acceleration power spectral density, run configuration 12

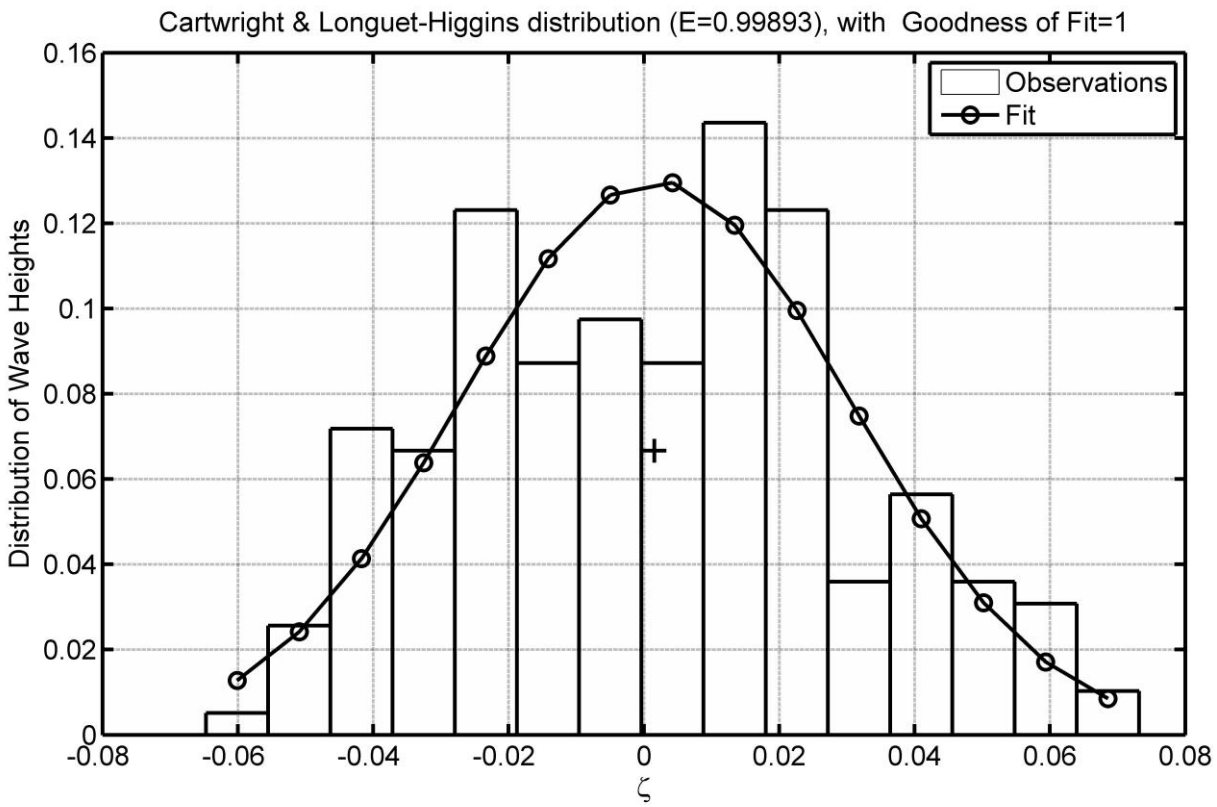

Figure 10: Example distribution of wave heights, run configuration 12

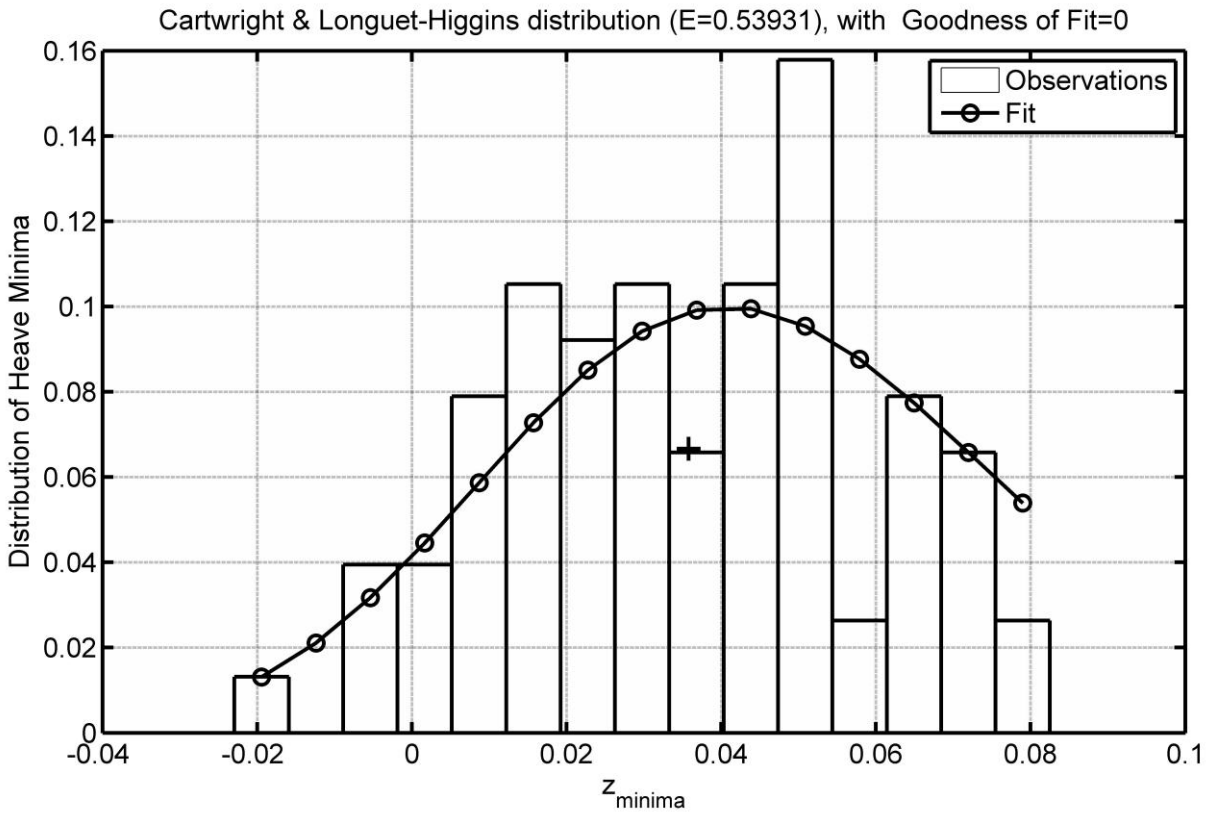

Figure 11: Example distribution of heave minima, run configuration 12

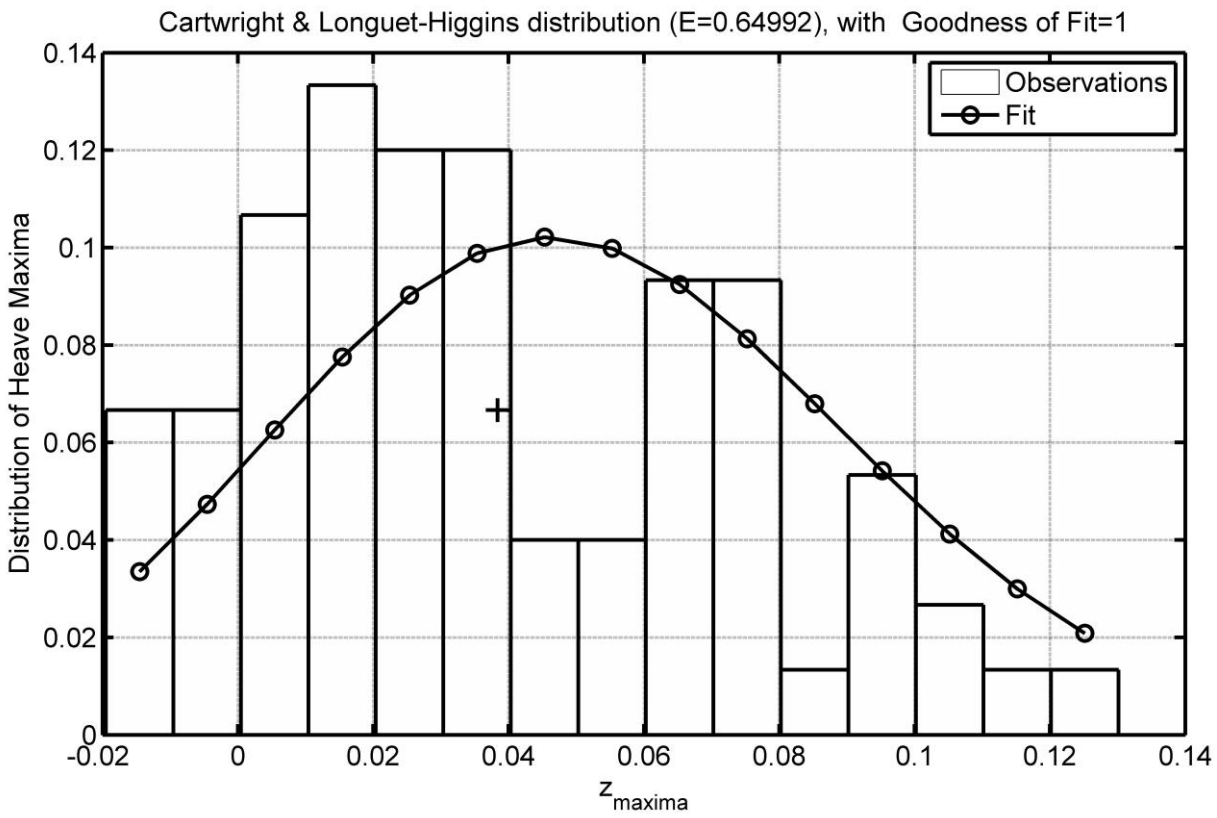

Figure 12: Example distribution of heave maxima, run configuration 12

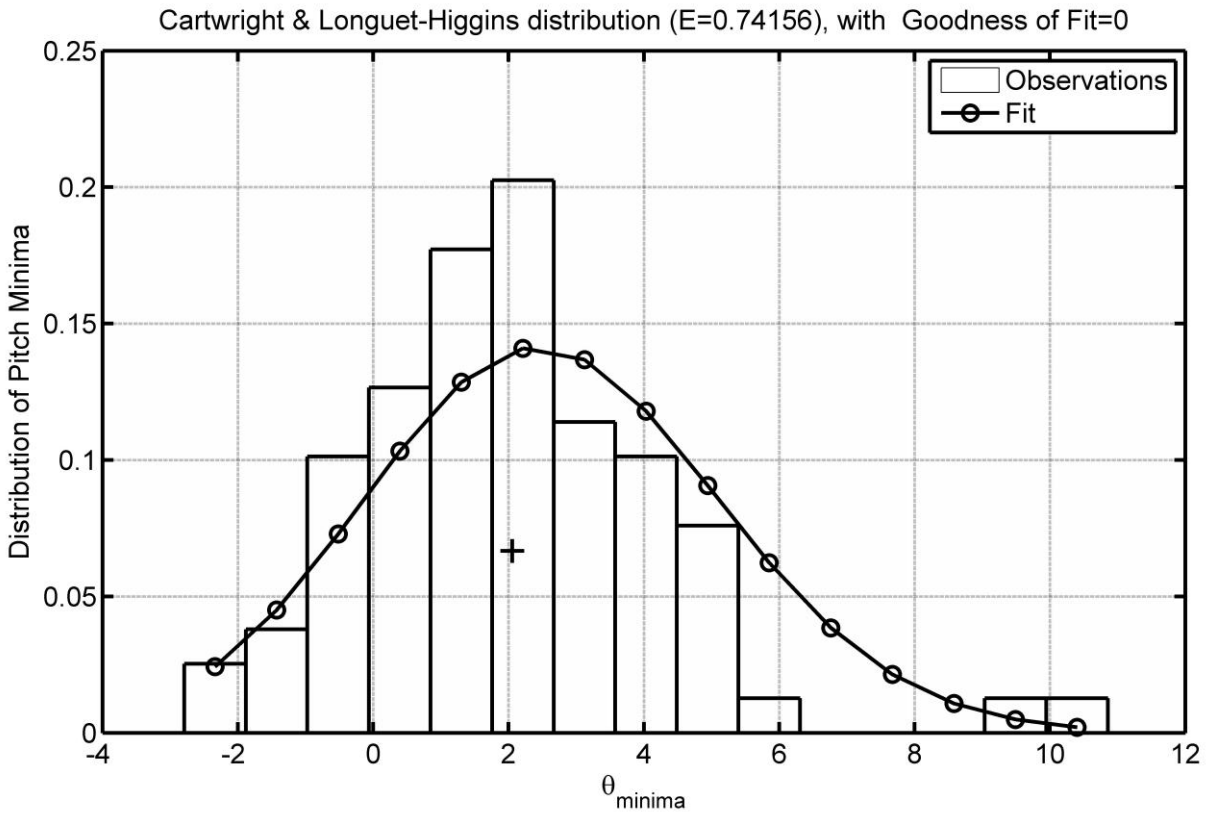

Figure 13: Example distribution of pitch maxima, run configuration 12

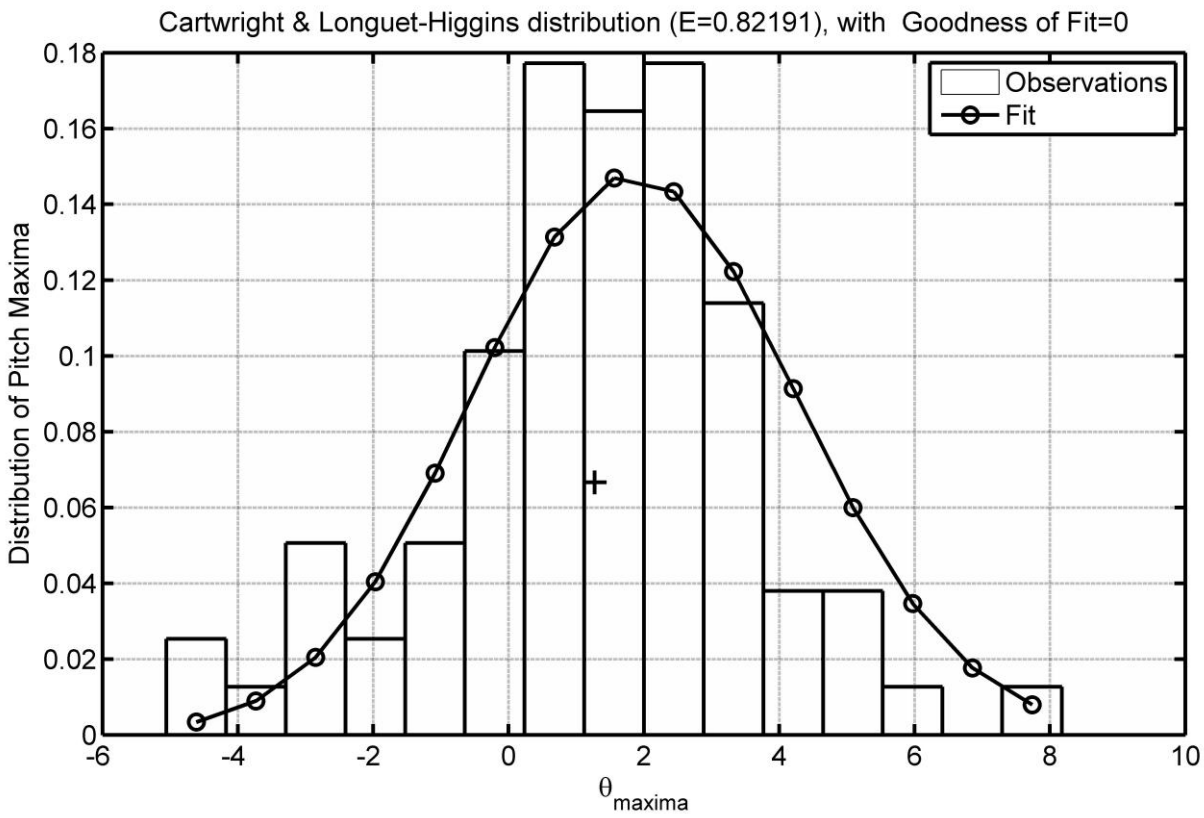

Figure 14: Example distribution of pitch minima, run configuration 12

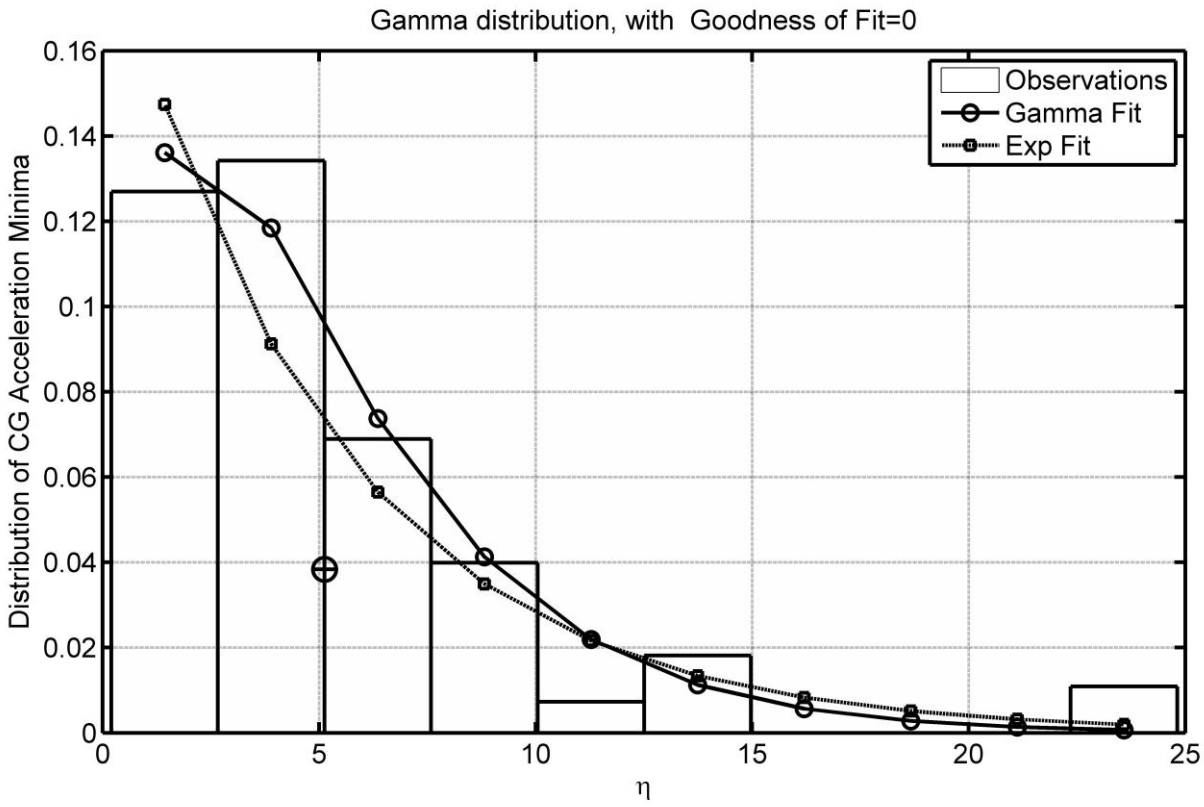

Figure 15: Example distribution of vertical accelerations minima at LCG, run configuration 12

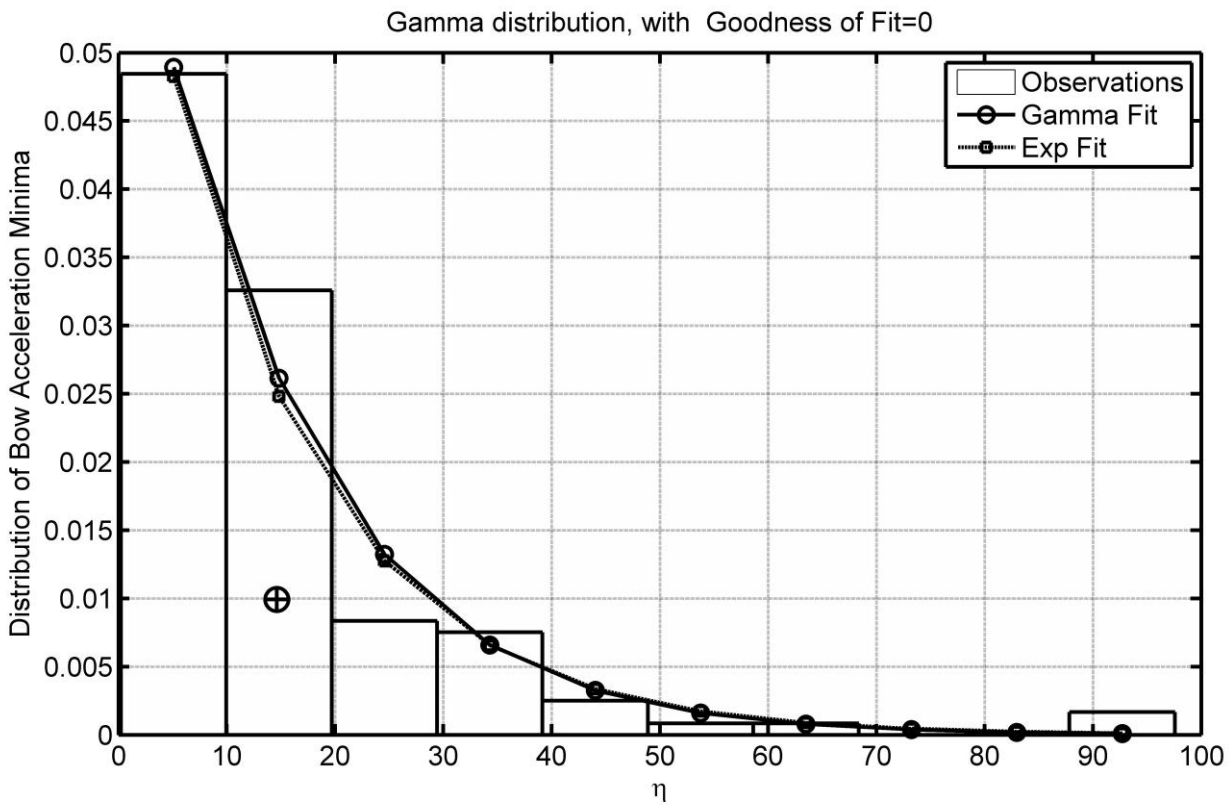

Figure 16: Example distribution of vertical acceleration minima at the bow, run configuration 12

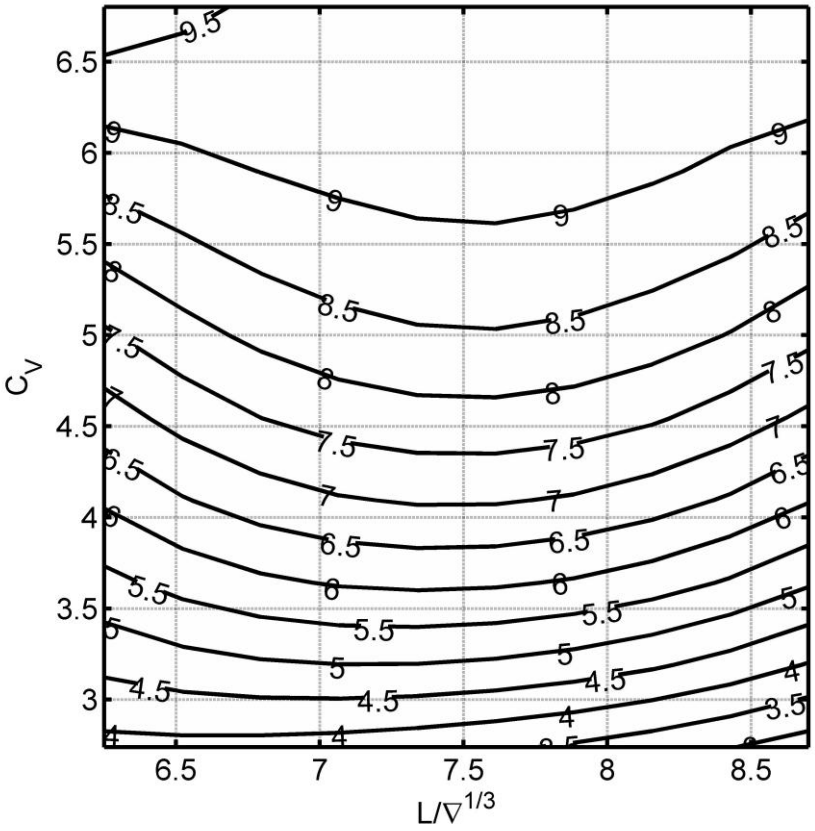

Figure 17: Linear regression model of Cv and $L/\nabla^{1/3}$ on RMS vertical accelerations at LCG [m/s^2].

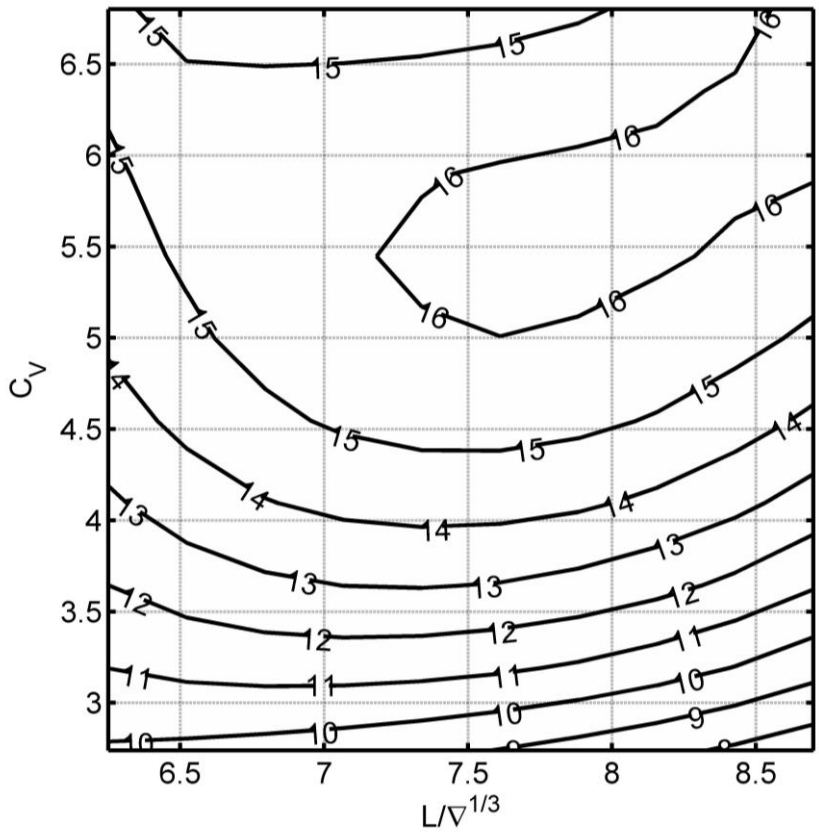

Figure 18: Linear regression model of Cv and $L/\nabla^{1/3}$ on RMS vertical accelerations at the bow [m/s^2].

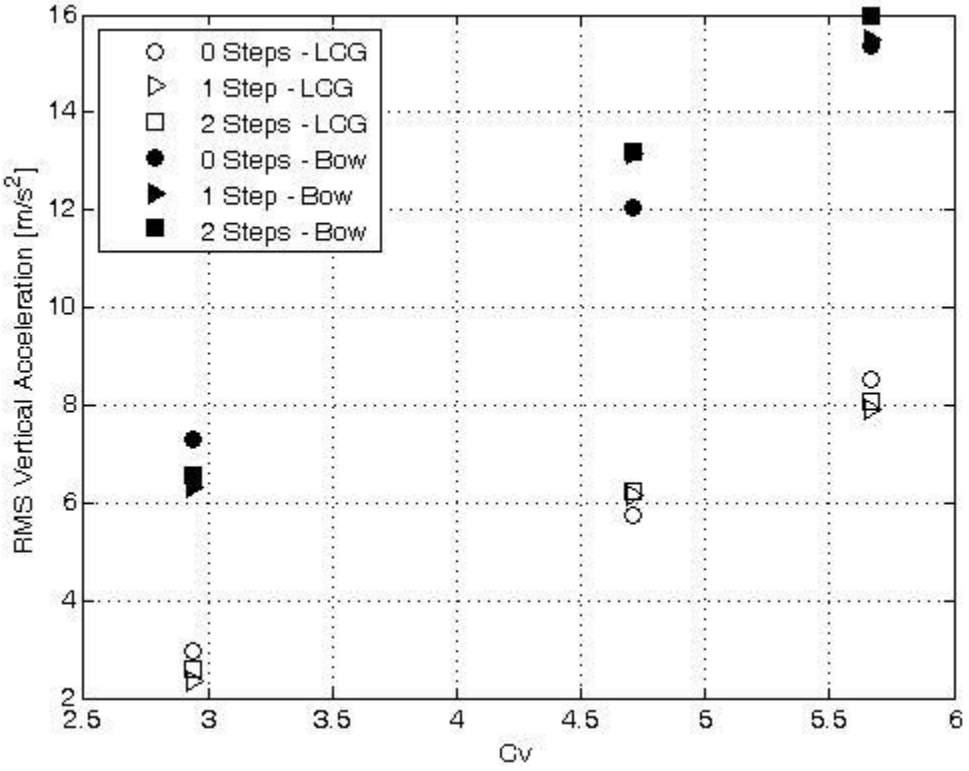

Figure 19: Influence of steps on the RMS vertical accelerations

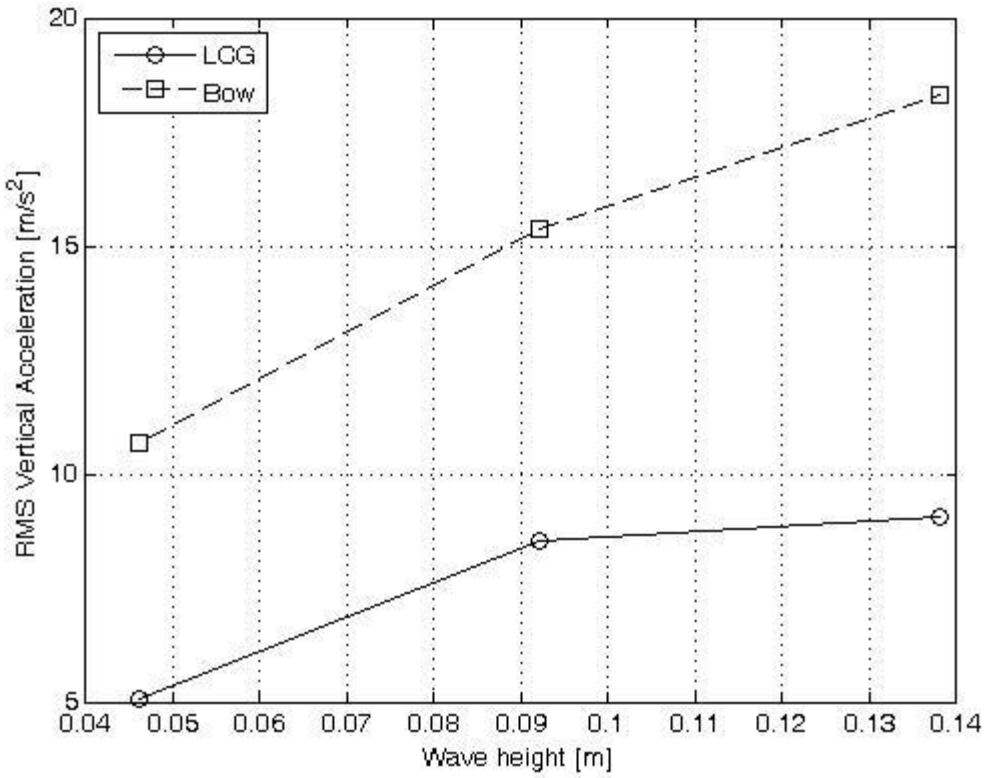

Figure 20: Influence of Wave height $H_{1/3}$ on the RMS acceleration of model C.